Electron. Mater. Lett.
DOI: 10.1007/s13391-017-6422-0

Optical Anisotropy in Micromechanically Rolled Carbon Nanotube Forest

Mohd Asyraf bin Mohd Razib,[1] Masud Rana,[1] Tanveer Saleh,[1,*] Harrison Fan,[2,3] Andrew Koch,[2] Alireza Nojeh,[2,3] Kenichi Takahata,[2] and Asan Gani Bin Abdul Muthalif[1]

[1]S3CRL Lab (Smart Structure, System, Control Research Laboratory), Mechatronics Engineering Department, Faculty of Engineering, International Islamic University Malaysia, Kuala Lumpur 50728, Malaysia
[2]Department of Electrical and Computer Engineering, University of British Columbia, Vancouver V6T 1Z4, Canada
[3]Quantum Matter Institute, University of British Columbia, Vancouver V6T 1Z4, Canada

(received date: 31 December 2016 / accepted date: 13 February 2017)

The bulk appearance of arrays of vertically aligned carbon nanotubes (VACNT arrays or CNT forests) is dark as they absorb most of the incident light. In this paper, two post-processing techniques have been described where the CNT forest can be patterned by selective bending of the tips of the nanotubes using a rigid cylindrical tool. A tungsten tool was used to bend the vertical structure of CNTs with predefined parameters in two different ways as stated above: bending using the bottom surface of the tool (micromechanical bending (M2B)) and rolling using the side of the tool (micromechanical rolling (M2R)). The processed zone was investigated using a Field Emission Scanning Electron Microscope (FESEM) and optical setup to reveal the surface morphology and optical characteristics of the patterned CNTs on the substrate. Interestingly, the polarized optical reflection from the micromechanical rolled (M2R) sample was found to be significantly influenced by the rotation of the sample. It was observed that, if the polarization of the light is parallel to the alignment of the CNTs, the reflectance is at least 2 x higher than for the perpendicular direction. Furthermore, the reflectance varied almost linearly with good repeatability (~10%) as the processed CNT forest sample was rotated from 0° to 90°.

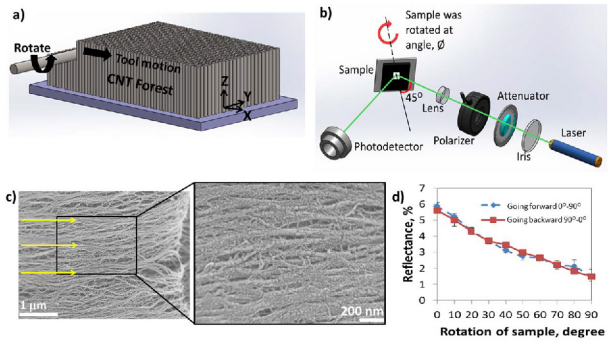

Keywords: carbon nanotube forest, micromechanical rolling, micromechanical bending, optical anisotropy, optical polarization

1. INTRODUCTION

Carbon nanotubes (CNTs) have drawn the interest of researchers worldwide, due to their outstanding physical,[1] electrical,[2] thermal[3] and optical properties.[4] Vertically aligned CNT arrays (CNT forests) have shown promise as a functional bulk material in MEMS[5] and other engineering applications.[6] Researchers have investigated many interesting optical properties of carbon nanotube forests. Kempa *et al*. in 2002 demonstrated photonic crystal effects from inexpensively fabricated, well-aligned CNTs.[7] Yang *et al*. and Mizuno *et al*. have shown that CNT forests have very high absorptivity[8,9] which is beneficial for the perfect optical absorption material application. Mukherjee *et al.* and Warsik *et al*. experimented with polarization-dependent reflection[10,11] from bare CNT forests across a wide range of the spectrum. In general, optical properties of CNT forests can be affected by both the properties of individual CNTs and their collective structural orientation.

To effectively use CNT forests for MEMS applications, many efforts have been made by researchers to produce bulk CNTs with patterns.[12,13] Patterning of CNT forests can be carried out either during the growth process with a pre-

*Corresponding author: tanveers@iium.edu.my

patterned catalyst or by different post processing techniques. Each has its advantages and disadvantages. The modification due to the post-patterning process could include transforming the two-dimensional (2-D) planar structure of bare CNT forests into free-form, three-dimensional (3-D) structures. One of such post processing techniques is to selectively bend the tips of the CNTs into the CNT forest. The tip bending of the CNTs can be carried out by a rigid rotating cylindrical tool; either by its bottom surface or by its peripheral surface. In our current study, we have shown that the second method (i.e. bending using the peripheral surface of the tool) aligns the CNTs linearly in the direction of motion of the tool. Furthermore, the optical characterization of the processed CNT forest zone revealed interesting anisotropic behavior, which we have reported in this letter.

2. FABRICATION PROCESS AND CHARACTERIZATION

2.1 CNT Forests Growth Process

The CNT forests used in this study were grown using an atmospheric-pressure chemical vapor deposition (CVD) system. Highly doped silicon substrates deposited with 10 nm of Alumina and 2 nm of Fe in thickness, respectively, were used as the base for the growth. The gasses (ethylene, hydrogen, and argon) were supplied with certain ratios, predefined time and temperature. The details of the VACNT array growth process can be found in a previous work by Saleh *et al.*.[14] This process mostly yielded forests of vertically aligned multiwall CNTs (diameters 30 nm to 50 nm) with lengths from 50 µm to several 100's of µm with total areas on the order of ~1 cm^2.

2.2 M2B (micromechanical bending) and M2R (micromechanical rolling) procedures

The M2B (micromechanical bending)[15,16] and M2R (micromechanical rolling) processes were performed using a servo-controlled 3-axis CNC Micromachining system (DT-110 Hybrid Mikrotools Ltd). The machine has a 1-µm positioning resolution. The schematic diagram in Figs. 1(a) & (b) illustrates the tip bending process of the CNTs using the methods of M2B and M2R, respectively (the arrows indicate the direction of the tool motion in the CNT forest). For the M2B method, the bottom surface of a rotating cylindrical shaft is used to bend the tips of the CNTs. Beforehand, wire-electro-discharge (WEDG)[17] was introduced to fabricate a micro shaft with 300 µm of diameter from the 500 µm original diameter to optimize the space usage on the bare CNT forest. The bottom surface of the 300 µm shaft was used for M2B processing. The bottom surface was fine finished by the WEDG process; the processing parameters were set at 90 V and 13 pF to ensure finest dimensions and surface finish are achieved on the bottom surface. The average surface roughness, Ra, was measured to be 0.422 µm using Alicona Infinite Focus Microscope G4. The shaft was programmed to rotate at a speed of 2000 rpm, which performed a translational motion in a uniaxial direction at a rate of 1 mm/min with a 1 µm step size into the CNT surface. These were the optimum parameters identified to produce the best surface roughness.[16] CNTs are compacted

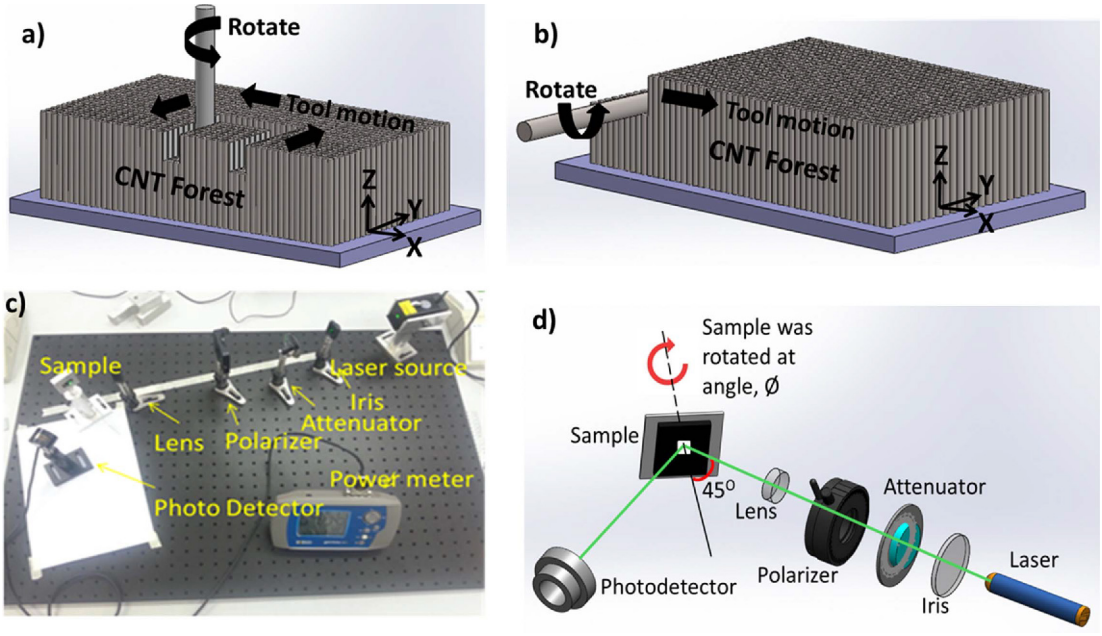

Fig. 1. a) & b) Concepts of M2B and M2R process, respectively, c) Experimental setup for optical characterization, d) Schematic diagram of c).

and bent by the bottom of the tool as stated earlier. On the other hand, for the M2R process, the circumferential surface of the rotating shaft (500 μm of diameter) was used to induce tip bending. The average surface roughness, Ra, was measured to be 0.102 μm for the circumference of the tool using Alicona Infinite Focus Microscope G4. In this case, the shaft was programmed to rotate at a speed of 5 rpm (significantly lower than in the M2B process, and comparable with[10]), which performed the translational motion in a uniaxial direction at a rate of 1 mm/h[10] on the CNT forest surface. CNTs are compacted and bent linearly by the side of the tool.

2.3 FESEM and Optical Characterization

The resultant processed zones of the CNT forest were studied using a JEOL JSM-6700F FESEM. Optical reflectance measurements were performed on the three samples, i.e., the bare CNT forest, the one processed by the M2B method and the one processed by the M2R method. An apparatus was set up, which consists of the laser source (partially polarized), attenuator, iris, polarizer, lens, samples and photodetector as shown in Fig. 1(c) and Fig. 1(d). The laser wavelength of 532 nm was chosen due to high reflectance in this region of wavelength.[18] The fully polarized laser (after the polarization filter) was targeted on the sample at a 45° incident angle. The polarizer was set so that only *p*-type polarized laser could pass through. Then the sample was rotated at angle Ø, 0° to 90° at 10° increments, forward and backward. Ø is the angle of rotation of the top surface of the CNT forest. The relationship between the sample's rotational angle, Ø and its reflectance was plotted. Experiments were conducted with the laboratory lights turned off. In addition, zero setting function (of the optical power meter) was used to offset the stray light so that the integrity of the results could be maintained. The experiment was repeated at least three times to ensure its repeatability.

3. RESULTS AND DISCUSSION

3.1 Bare CNT Forests

Bare CNT forests (VACNT arrays) are highly porous materials with entanglement at the top end as shown in Fig. 2(a). Because of the porosity of the CNT forest, the incident light easily penetrates into the bulk CNT material and is absorbed by the array.[16] The two post processing methods of VACNT arrays, namely M2B and M2R, bend the tips of VACNTs selectively to close the gaps at the top of the CNT forest (which are due to its inherent porosity). Therefore, the M2B and M2R processed CNT forests reflect light significantly better than the bare CNT forest. However, M2B

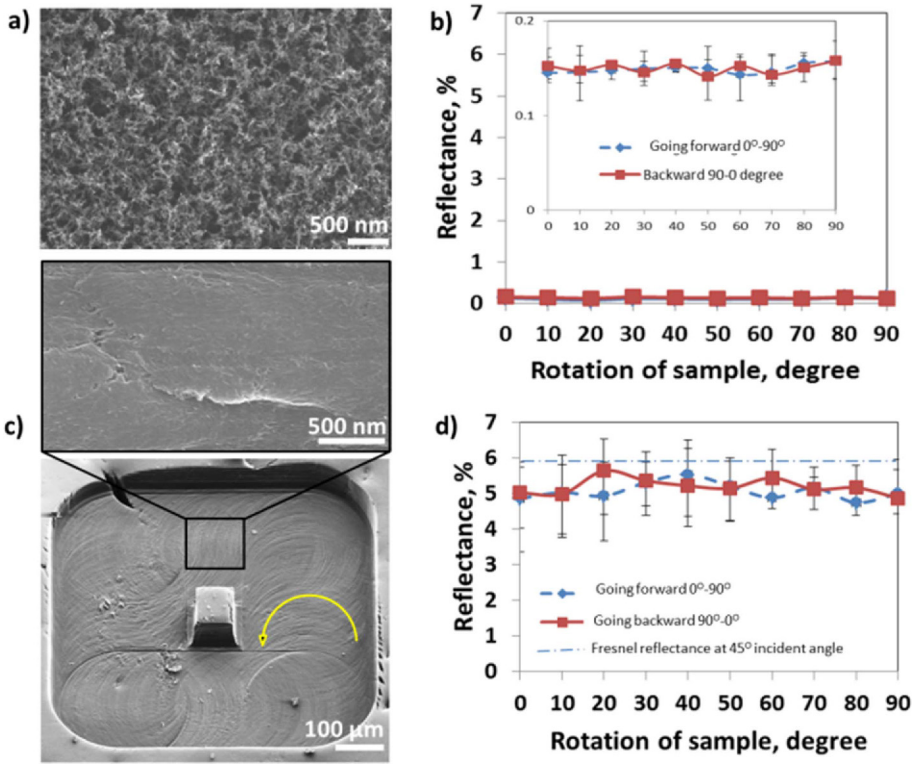

Fig. 2. a) FESEM image of top of bare CNT forest b) Optical reflectance against rotation angle of the sample, Ø, between 0 and 90° of bare CNT forest c) FESEM image of top of M2B-processed CNT forest d) Optical reflectance against rotation angle of the sample, Ø, between 0 and 90° of M2B-processed CNT forest. Error bars are also shown to indicate the maximum and minimum measured reflectance values.

and M2R processes generate different surface textures, which show dissimilar responses to the incident polarized laser. Figure 2(b) shows an attempt to measure the reflectance on the rotating bare CNT forests at a fixed 45° incident angle. The measured value was notably low with an average reflectance of around ~0.15-0.16%. The value is comparable with the previously reported data on bare CNT forests, having a 0.045% reflectance at normal incidence.[8] Our value is slightly higher due to the higher incident angle i.e. 45°, as predicted by the Fresnel equation (equation (1)). Another observation from the plot in Fig. 2(b) is that the reflectance changes marginally and randomly with the rotation of the sample due to the isotropic bare CNT forest surface.

3.2 M2B-processed surface

With the M2B method, the surface was deformed with overlapping trochoidal patterns. The arrow in Fig. 2(c) shows the direction of alignment of the patterned CNT forests. This phenomenon was explained in our earlier work.[16] Figure 2(c) (with higher magnification image) suggests that the gaps of the top surface have been closed because of the M2B process. Thus there is an increase of reflectance from the M2B-processed surface. Previously Asyraf *et al*.[16] reported that the surface roughness achieved by this process could be as low as 15 nm with optimized parameters. Figure 2(d) reveals that the reflectance from the M2B-processed CNT forest surface was on average ~4.5-5.5%. Saleh *et al.*[19] reported earlier that the reflectance of unpolarized light from an M2B-processed CNT forest surface was 10-15%. However, in this study, we achieved lower reflectance (almost 2 x) from the same surface with a p-polarized green laser. Again, the Fresnel equation for the reflectance of p-polarized light (equation (1)) can be used to verify the results for a wavelength of 532 nm at a 45° incidence angle (as used for this study):

$$R_p = \left|\frac{n_1\cos\theta_t - n_2\cos\theta_i}{n_1\cos\theta_t + n_2\cos\theta_i}\right|^2 = \left|\frac{n_1\sqrt{1-\left(\frac{n_1}{n_2}\sin\theta_i\right)^2} - n_2\cos\theta_i}{n_1\sqrt{1-\left(\frac{n_1}{n_2}\sin\theta_i\right)^2} + n_2\cos\theta_i}\right|^2 \quad (1)$$

R_p: reflectance of p-polarized light
n_1: refractive index for first medium, air
n_2: refractive index for second medium, patterned CNT forest
θ_i: incident angle
θ_t: transmittance angle

The value of the refractive indices of air and unprocessed CNT forests can be considered to be 1.00293[20] and 1.04,[21] respectively. R_p can be calculated from equation (1) for various values of θ_i if a value of refractive index for the processed CNT forest is assumed. Figure 3 shows the simulated and experimental values of R_p as a function of incident angle for the M2B-processed surface. The refractive index of the tip bent CNT forest is assumed to be 2.2 for best fitting the experimental and simulated values of R_p. At a 45° incident angle (this is our incident angle for subsequent experiments) R_p was calculated to be ~5.81% (from equation (1); also shown in Fig. 2(d)), which is comparable with our experimental results (average ~5.08%) with the 532 nm wavelength green laser. The experimental value is slightly lower, which could be due to small pits and holes on the M2B-processed surface. Again, another important observation from Fig. 2(d) is that the reflectance from the M2B-processed surface does not show any obvious correlation with the rotation angle, Ø, of the sample. The reason behind the above observation is the circular alignment of the CNTs on the resulting surface of the VACNTs array as shown in Fig. 2(c).

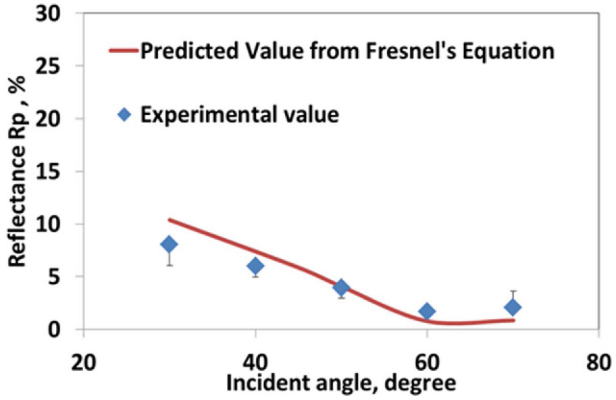

Fig. 3. The simulated and experimental value of reflectance, R_p, for the M2B-processed CNT forest. Error bars are also shown to indicate the maximum and minimum measured reflectance values.

3.3 M2R-processed surface

Figure 4(a) shows a high-resolution FESEM image of the M2R-processed CNT forest surface. It can be understood from comparison between FESEM images, Fig. 2(c) and Fig. 4(a), that the M2R process aligns the CNTs more linearly in the direction of motion of the tool. Previous attempts were also made to produce straight alignment of CNTs parallel to the substrate. De Heer *et al.*[22] used a metal plate to shear CNTs to bend in the same direction. In another attempt, a compressive force (~1 kg) was applied to the roller to produce different levels of bending.[10]

A very interesting characteristic of the M2R- processed CNT forest surface is its optical response to the incident polarized light, as shown in Fig. 4(b). The reflectance test of the M2R-processed sample was carried out similarly to that

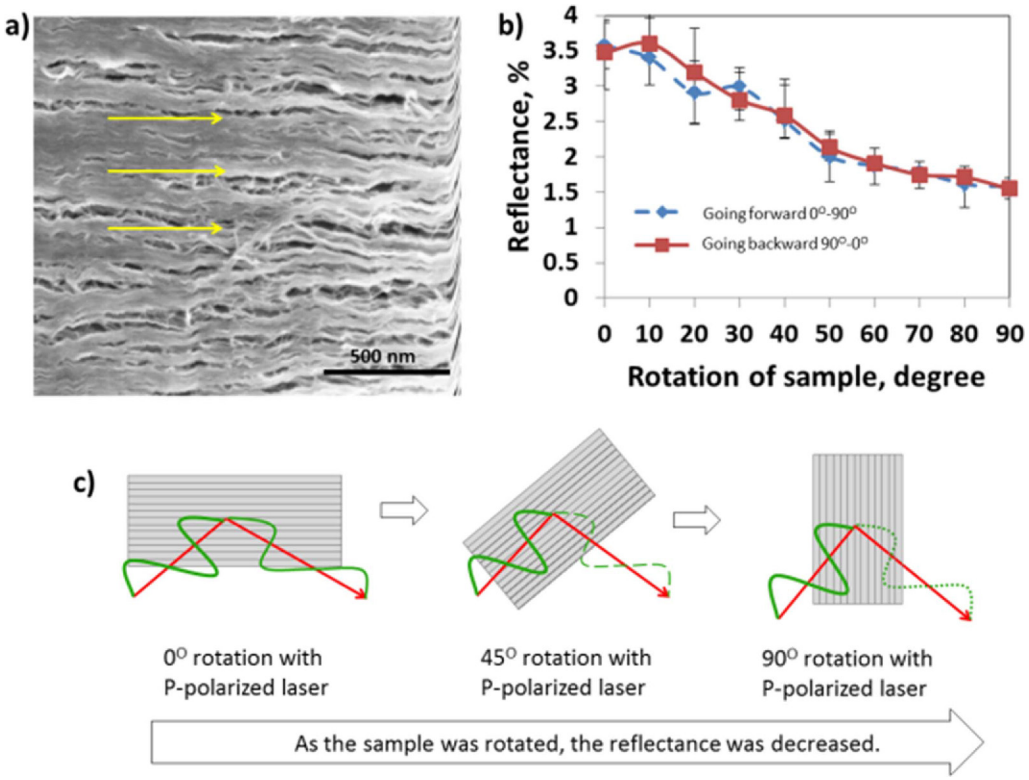

Fig. 4. a) FESEM image of the M2R-processed sample with the arrow direction showing the alignment of the CNTs. b) Optical reflectance against rotation angle of the sample between 0° and 90°. c) Concept of polarized laser reflectance against the the anisotropic surface. Error bars are also shown to indicate the maximum and minimum measured reflectance values.

for the bare CNT forest and the M2B-processed CNT forest.

Interestingly, it was observed that the reflectance of p-polarized laser decreases almost linearly from 3.5% to 1.5% as the sample is rotated at angle Ø from 0° to 90°. The CNTs are aligned parallel to the plane of incidence when the sample is at 0°. On the other hand, the electric field of the p-polarized laser is completely perpendicular to CNTs' alignment as the sample is positioned at 90°. De Heer[22] reported earlier that aligned CNTs behave anisotropically, showing higher dielectric function (hence high reflectance) along the CNTs compared to the perpendicular direction during ellipsometry. A similar observation was also made in this study, and higher reflectance was observed when the nanotubes were parallel to the plane of incidence as explained in Fig. 4(c). However, in this paper, we report for the first time how the reflectance is varied with continuous rotation of the M2R processed sample. It is understandable from Fig. 4(a) that the CNTs were aligned linearly in the direction of the tool motion during the M2R process. The resultant surface has some cracks which may cause low reflectance and non-repeatable data.

3.4 M2R-processed surface with gold coating

To improve the situation by increasing the reflectance from the M2R processed sample, we attempted gold (Au) coating onto the surface of the patterned CNT forests. To maintain the M2R-processed CNT forest's anisotropic behavior, we tried a very thin layer of coating on the surface, at approximately 15 nm,[23] using a JOEL JFC-1600 ion magnetron sputtering machine. Coating of different materials onto the CNT has been previously attempted, with the intention to enhance its properties. Mukherjee *et al.*[24] performed coating of Aluminum (Al) onto CNT films to enhance their reflection from ~15% to ~65% across a wide range of the optical spectrum (500-2500 nm). Gold was chosen for this study because the reflectance of the 532 nm laser wavelength is higher for gold as compared to aluminum (Al) and silver (Ag).[25] A thin coating of Au on the CNTs not only presented the enhancement of the optical reflectance but interestingly preserved the alignment of the CNTs: the surface morphology in Fig. 5(a) shows the alignment is still intact. The enlarged view shows signs of gold spots on the CNTs. Figure 5(b) indicates that the reflectance is increased when compared with Fig. 4(b) by more than 1.5 times when the sample is positioned at 0°. The reflectance value decreases from ~6% to 1.5% with the rotation, Ø, of the sample. This change provides evidence that the anisotropic behaviour of the M2R-processed sample

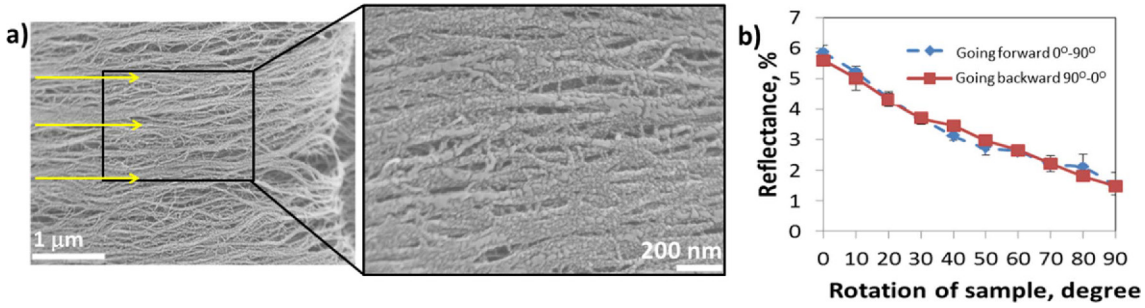

Fig. 5. a) FESEM of Au-coated CNT forest patterned by the M2R method. b) Optical reflectance of the sample shown in (a) against rotation angle, Ø, between 0° and 90°. Error bars are also shown to indicate the maximum and minimum measured reflectance values.

is still maintained.

4. CONCLUSIONS

In this letter, we have presented a process called micromechanical rolling (M2R) to align the CNTs linearly in a VACNT array. The process enhances the optical reflectance of the VACNT array and, more interestingly, the reflectance was observed to be a function of the angular position of the sample. We investigated three different types of samples. For the M2R-processed sample without any reflective coating, the observed reflectance at 0° of rotation angle was 3.5%. However, when the sample was coated with a very thin layer of gold (Au) (~15 nm), the reflectance was increased by 1.5 × times. Nonetheless, the anisotropic behavior of the sample was preserved. The finding from this study will open opportunities to develop new types of angle sensors based on M2R-processed VACNT arrays.

ACKNOWLEDGEMENTS

This work was supported by MOSTI (SF14-008-0058) and MOHE (FRGS13-083-0324). K. Takahata is supported by the Canada Research Chairs program. A. Nojeh and K. Takahata thank the Natural Sciences and Engineering Research Council of Canada (SPG-P 478867). The authors are grateful to IIUM, UPSI, UiTM and MIMOS for providing machining and testing facilities to carry out the experiments and all their valuable support to carry out this research work. This research was undertaken thanks in part to funding from the Canada First Research Excellence Fund, Quantum Materials and Future Technologies Program.

REFERENCES

1. K. T. Kashyap and R. G. Patil, *Bull. Mater. Sci.* **31**, 185 (2008).
2. M. Park, B. A. Cola, T. Siegmund, J. Xu, M. R. Maschmann, T. S. Fisher, and H. Kim, *Nanotechnology* **17**, 2294 (2006).
3. Y. Fu, N. Nabiollahi, T. Wang, S. Wang, Z. Hu, B. Carlberg, Y. Zhang, X. Wang, and J. Liu, *Nanotechnology* **23**, 45304 (2012).
4. S. B. Tooski, A. Godarzi, M. S. Solari, M. Ramyar, and A. Roohforouz, *J. Appl. Phys.* **110**, 34307 (2011).
5. Y. Q. Jiang, Q. Zhou, and L. Lin, *Proc. 2009 IEEE 22nd International Conference on Micro Electro Mechanical Systems (MEMS)*, p. 587, IEEE, Sorrento, Italy (2009).
6. Y. Jiang, A. Kozinda, T. Chang, and L. Lin, *Sensor. Actuat. A-Phys.* **195**, 224 (2013).
7. K. Kempa, B. Kimball, J. Rybczynski, Z. P. Huang, P. F. Wu, D. Steeves, M. Sennet, M. Giersig, D. V. G. L. N. Rao, D. L. Carnahan, and D. Z. Wang, *Nano Lett.* **3**, 13 (2003).
8. Z. P. Yang, L. Ci, J. A. Bur, S. Y. Lin, and P. M. Ajayan, *Nano Lett.* **8**, 446 (2008).
9. K. Mizuno, J. Ishii, H. Kishida, Y. Hayamizu, S. Yasuda, D. N. Futaba, M. Yumura, and K. Hata, *Proc. Natl. Acad. Sci. U. S. A.* **106**, 6044 (2009).
10. S. Mukherjee and A. Misra, *J. Phys. D: Appl. Phys*. **47**, 235501 (2014).
11. M. Wąsik, J. Judek, and M. Zdrojek, *Carbon* **64**, 550 (2013).
12. F. C. Cheong, K. Y. Lim, C. H. Sow, J. Lin, and C. K. Ong, *Nanotechnology* **14**, 433 (2003).
13. B. Q. Wei, R. Vajtai, Y. Jung, J. Ward, R. Zhang, G. Ramanath, and P. M. Ajayan. *Chem. Mater.* **15** 1598 (2003).
14. T. Saleh, M. Dahmardeh, A. Bsoul, A. Nojeh, and K. Takahata, *J. Appl. Phys.* **110**, 103305 (2011).
15. M. A. M. Razib, T. Saleh, and M. Hassan, *Smart Instrumentation, Measurement and Applications (ICSIMA), 2014 IEEE International Conference,* pp. 25-27, IEEE, Kuala Lumpur, Malaysia (2014).
16. M. R. Mohd Asyraf, M. Masud Rana, T. Saleh, Harrison D. E. Fan, Andrew T. Koch, A. Nojeh, K. Takahata, and A. B. Suriani. *Fuller. Nanotub. Car. N.* **24**, 88 (2016).
17. T. Masuzawa, M. Fujino, K. Kobayashi, T. Suzuki, and N. Kinoshita, *CIRP Ann. - Manuf. Techn.* **34**, 431 (1985).
18. X. J. Wang, J. D. Flicker, B. J. Lee, W. J. Ready, and Z. M. Zhang, *Nanotechnology* **20**, 215704 (2009).

19. T. Saleh, M. V. Moghaddam, M. S. M. Ali, M. Dahmardeh, C. A. Foell, A. Nojeh, and K. Takahata, *Appl. Phys. Lett.* **101**, 61913 (2012).
20. J. C. Owens, *Appl. Opt.* **6**, 51 (1967).
21. H. Shi, J. G. Ok, H. Won Baac, and L. Jay Guo, *Appl. Phys. Lett.* **99**, 211103 (2011).
22. W. A. deHeer, W. S. Bacsa, A. Châtelain, T. Gerfin, R. Humphrey-Baker, L. Forro, and D. Ugarte, *Science* **268**, 845 (1995).
23. T. Saleh, A. N. Rasheed, and A. G. A. Muthalif, *Int. J. Adv. Manuf. Tech.* **78**, 1651 (2015).
24. S. Mukherjee, A. Suri, V. K. Vani, and A. Misra, *Appl. Phys. Lett.* **103**, 131909 (2013).
25. M. A. Ordal, L. L. Long, R. J. Bell, S. E. Bell, R. R. Bell, R. W. Alexander, and C. A. Ward, *Appl. Opt.* **22**, 1099 (1983).